Hindawi
Advances in Materials Science and Engineering
Volume 2018, Article ID 6153252, 12 pages
https://doi.org/10.1155/2018/6153252

Research Article

Comparison of Pentaerythrotol and Its Derivatives as Intumescent Flame Retardants for Polypropylene

Siwen Huang, Jiayou Xu, Haiming Deng, Jie Liu, and Yuanfang Xiao

School of Chemistry & Chemical Engineering, Guangzhou University, Guangzhou 510006, China

Correspondence should be addressed to Jiayou Xu; xujiayou516@163.com

Received 14 March 2018; Accepted 24 July 2018; Published 28 August 2018

Academic Editor: Peter Majewski

Hydroquinol bis[di(2,6,7-trioxa-phosphabicyclo[2.2.2]-octane-1-oxo-4-hydroxylmethyl)]phosphate (PBPP), which contains caged phosphates and benzene groups, was synthesized. The caged phosphate structure of PBPP was characterized by Fourier transform infrared spectroscopy (FT-IR), hydrogen nuclear magnetic resonance (^{1}H-NMR), and phosphorus nuclear magnetic resonance (^{31}P-NMR). The experimental results showed that PBPP had better performance than 1-oxo-4-hydroxymethy1-2,6,7-trioxa-1-phosphabicyclo[2.2.2]-octane (PEPA) and pentaerythritol (PER) in water resistance, compatibility with polypropylene (PP), thermal stability, and flame retardancy of intumescent flame retardant PP (IFR-PP) systems. It was attributed to the symmetrical structure and stereohindrance effect of PBPP. The IFR-PP systems reached UL94 V-0 flammability rating when the minimal addition of IFR with PBPP, PEPA, or PER was 25%, 23%, and 28%, respectively. The flame retardant mechanisms of IFR containing PBPP, PEPA, and PER were investigated by FT-IR and scanning electron microscopy (SEM). PBPP formed a perfect charring layer, with the high carbon content of PBPP helping it form the charring layer more quickly.

1. Introduction

PP is one of the most widely used thermoplastics in lots of fields, such as automobiles, electrical appliances, and as building materials, because of its low cost, good chemical resistance, and ease of processing [1–5]. However, the use of PP is still limited for some applications due to its inflammability. Therefore, it is desirable to improve the flame retardant property of PP. Halogen-containing compounds can be used as flame retardant additives in PP, but their applications are restricted because of the emission of corrosive and toxic gases when the material burn [6, 7]. Additionally, metal hydroxides are another kind of flame retardant additive in PP. But they require high loading and have poor compatibility with the polymer matrix which have severely limited their application in PP [8].

Recently, intumescent flame retardants (IFRs) have attracted more and more attention and have been regarded as the most promising additives to displace halogen-containing flame retardants because they produce low smoke and no toxic or corrosive gases [9–20]. The IFR system is generally composed of three ingredients, i.e., an acid source, a charring agent, and a blowing agent [12, 14, 17, 18]. The earliest IFR system, consisting of ammonium polyphosphate (APP), pentaerythritol (PER), and melamine (MEL), has been systematically studied by Camino and coworkers [21–24]. However, the low water resistance of PER, due to its four hydroxyl groups, leads to a severe deterioration of the flame retardancy [25–28].

In 1960s, Verkade et al. firstly synthesized 1-oxo-4-hydroxymethy1-2,6,7-trioxa-1-phosphabicyclo[2.2.2]-octane (PEPA) [29]. In the 1980s, Halpern et al. [30] first used PEPA and its derivatives as a flame retardant of polyolefins. It was found that these compounds had good char-forming ability and thermal stability when they were used as both a carbon and acid source. Moreover, the Borg-Warner Chemical Co., Ltd. synthesized caged phosphate melamine salts based on PEPA [31, 32]. Ou and his coworkers [4] synthesized a caged aliphatic phosphate, tri(2,6,7-trioxa-1-phosphabicycle[2,2,2]-octane-1-oxo-40methanol)phosphate (Tri-mer), from PEPA which had good thermal stability and flame retardant properties in PP. Chiu and Wang designed and synthesized

a caged phosphate ester containing sulfur which had excellent flame retardancy in PP [9]. To the best of our knowledge, studies on the derivatives of PEPA have been the hot point. These works pay much effort to modify PEPA to improve its hydrophobicity. Hydroquinone is capable of endowing active end-functional groups (-OH) which can participate in the construction of derivatives of PEPA. Furthermore, benzene groups in hydroquinone can improve the carbon content of the charring agent. So, we present a scheme for synthesizing a caged phosphate structure by improving the carbon and phosphorus content and the stereohindrance effects.

In this paper, a charring agent, PBPP, was synthesized from PEPA, phosphorus oxychloride ($POCl_3$), and hydroquinone. The structure of PBPP was characterized by FT-IR, ^{1}H-NMR, and ^{31}P-NMR. The compatibility with PP and the effects of PBPP, PEPA, and PER on the water resistance, thermal degradation, flame retardancy of intumescent flame retardant of PP (IFR-PP) systems, and the IFR flame retardant mechanism were also been investigated by thermogravimetric analysis (TGA), UL-94 test, cone calorimetry test, Fourier transform infrared spectroscopy (FT-IR), and scanning electron microscopy (SEM).

2. Experimental

2.1. Materials. 1-oxo-4-hydroxymethy1-2,6,7-trioxa-1-phosphabicyclo[2.2.2]-octane (PEPA) was purchased from Jiangsu Victory Chemical Co., Ltd., China. Phosphorus oxychloride ($POCl_3$) (AR) was supplied by Wuhan Yuancheng Technology Co., Ltd., China. Hydroquinone ($C_6H_4(OH)_2$) (AR) was obtained from the Jining Hongming Chemical Reagent Co., Ltd., China. Acetonitrile, triethylamine, and ethanol were obtained form the Tianjin Zhiyuan Chemical Reagent Co., Ltd., China. PP (PPH-T03) was offered by Sinopec Beihai Petrochemical Co., Ltd., China. Ammonium polyphosphate (APP) was bought from Jinhua Tianyuan Chemical Industry, China.

2.2. Preparation

2.2.1. Synthesis of PPPC. $POCl_3$ (0.20 mol) and acetonitrile (50 ml) were added into a 500 mL four-neck flask equipped with a mechanical stirrer, an addition funnel, a condenser, and a tail gas absorber and stirred at 60~65°C. Both PEPA (0.40 mol) and acetonitrile (250 ml), each divided into five parts, were added into the above flask. Thereafter, the mixture was refluxed for about 22 h after being heated to 85~90°C. The mixture was then cooled to room temperature, and the precipitate was filtered and washed with acetonitrile. The white, dried solid (PPPC) was obtained (yield: 89.5%). The synthesis route is shown in Scheme 1.

2.2.2. Synthesis of PBPP. In another, similar 500 mL four-neck flask, PPPC (0.12 mol) and acetonitrile (100.00 ml) were added. Then, hydroquinone (0.06 mol), triethylamine (0.12 mol), and acetonitrile (100.00 ml) were simultaneously added dropwise to the flask at room temperature. The mixture was heated to 60~65°C and stirred for about 30 min.

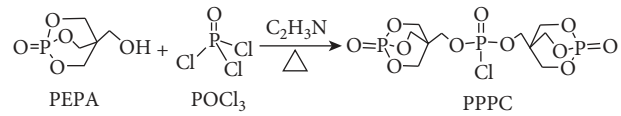

Scheme 1: Synthesis of PPPC.

Thereafter, the mixture was kept at 90~95°C and refluxed for 6 h. The precipitate was then filtered and washed with acetonitrile. The product was dried for 12 h at 100°C to give PBPP as a white powder (yield: 23.42%). The synthesis route is shown in Scheme 2.

2.2.3. Preparation of Flame-Retardant PP Samples. Mixing appropriate amount of PP, APP, and the charring agent (PER, PEPA, or PBPP) on a two-roll mill at about 180°C at a rotor speed of 60 rpm for 8 minutes for each sample prepared PP composites. Then, the composites were transferred to a mold preheated for 5 minutes at 180°C and pressed at 10 MPa followed by cooling to room temperature while keeping the same pressure for 5 minutes. The sample's sheets obtained with a suitable size were for analysis.

2.3. Characterization. PBPP, PEPA, PER, and the residual char, obtained at different temperatures muffle furnace, were characterized by FT-IR. The measurements were performed on a Nicolet 6700 FT-IR (Nicolet Instrument Company, USA) spectrometer by using KBr pellets.

Vertical burning tests were carried out by using a CZF-2 vertical burning test instrument produced by Jiangning Analysis Instrument Factory, China, with sheet dimensions of 127 mm ×12.7 mm × 3.2 mm, according to ASTM D3801. Cone calorimeter tests were performed by using a FTT cone calorimeter at a heat flux of 5×10^{-2} kW·m^{-2}, according to ISO 5660-1. The size of the samples was 100 mm × 100 mm × 3.2 mm.

TGA was carried out with a TA SDTQ600 thermal analyzer from 25°C to 700°C at a heating rate of 20°C·min^{-1} in air conditions for all samples.

SEM was used to investigate the morphology of the PBPP/PP, PEPA/PP, PER/PP without burning, and the char residue of the IFR-PP systems after the cone calorimeter tests.

3. Results and Discussion

3.1. Characterization of PBPP. Figure 1 shows the FTIR spectra of PER (a), PEPA (b), and PBPP (c). The peaks of PEPA and PER at 3388 cm^{-1} are associated with ν_{OH}. However, there were no obvious peaks at 3388 cm^{-1} for PBPP. It indicates that there were no hydroxy groups in the structure of PBPP. The absorption band at 3001 cm^{-1} corresponds to $\nu_{C\text{-}H}$ of the benzene rings of PBPP and that at 2914 cm^{-1} assigned to $\sigma_{C\text{-}H}$ of PEPA. Moreover, the peaks at 1645 cm^{-1} and 1470 cm^{-1} can be assigned to $\nu_{C=C}$ of benzene rings and the peaks at 1313 cm^{-1} are associated with $\sigma_{P=O}$. The absorption bands at 1027 cm^{-1} are $\sigma_{P\text{-}O\text{-}C}$, and the absorption bands at 854 cm^{-1} are assigned to the skeleton

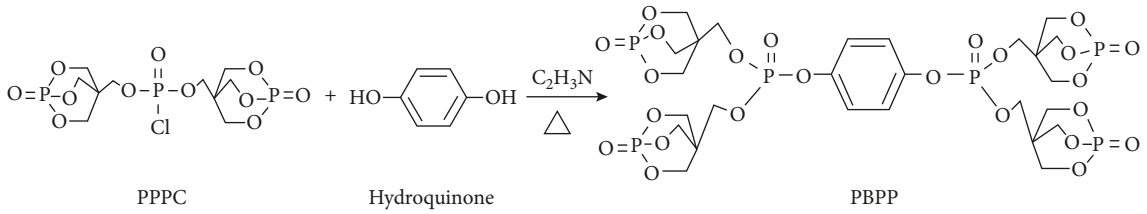

Scheme 2: Synthesis of PBPP.

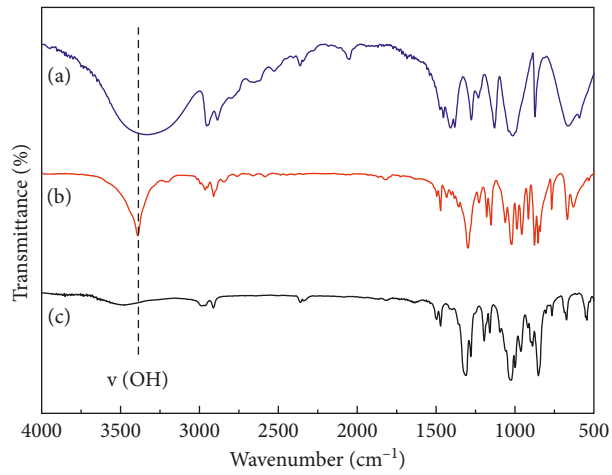

Figure 1: The FT-IR spectra of PER (a), PEPA (b), and PBPP (c).

vibration of caged bicycle phosphates. The appearance of the characteristic absorption bands of benzene and PEPA indicate that PBPP was successfully synthesized.

Figure 2 shows the ^{1}H-NMR spectrum of PBPP. Peaks at 6.57 ppm are assigned to aromatic protons (a). In addition, a peak at 4.64 ppm can probably be attributed to the -CH_2- protons (b) from the caged bicyclic phosphates. The -CH_2- protons (c) are at 3.99 ppm, which are near to the caged ring resonate. Based on ^{1}H-NMR, successful synthesize of PBPP was confirmed.

The structure of PBPP was also characterized by ^{31}P-NMR spectra, as shown in Figure 3. Two sharp signals were observed. The sharp peak at 7.96 ppm indicated the phosphorus from the caged bicyclic phosphates and the phosphorus linked with hydroquinone. The other two sharp peaks, at 1.48 ppm, showed that there were by-products in the sample, which contained two-caged bicyclic phosphates or one-caged bicyclic phosphate. All of these results prove that the target product was successfully synthesized.

3.2. Water Resistance of PBPP, PEPA, and PER. Since PER and PEPA are rich in hydroxyl groups, it is easy to migrate from composite and dissolve in water, resulting in loss of flame retardancy. In this work, the derivatives (PBPP) of PEPA were synthesized, with the goal of improving water resistance. Therefore, their water resistance experiment needs to be done. Digital photos and graphs of PER (a), PEPA (b), and PBPP (c) (1 g each) dissolved in H_2O (5 ml) are illustrated in Figure 4. The PER gets dissolved in the water easily due to its four hydroxyl groups. PEPA is also a hydrophilic substance, because of its hydroxyl group, but was less soluble than PER. However, PBPP could be well dispersed in H_2O attributed to there being no hydroxyl group in the structure of PBPP. Moreover, the solubility of PBPP was the least of the three at all temperatures. When the temperature was increased, the solubility of PER reached its peak maximum of 0.8 g. The solubility of PER at 80°C was twice more than that of PBPP. All of these results indicated that PBPP had the better water resistance than PEPA and PER.

3.3. Compatibility of PER, PEPA, and PBPP with PP. Generally, the compatibility between filler and PP are studied by SEM observation of the fracture surface of PP composites. Figure 5 shows the SEM images of PP/PER, PP/PEPA, and PP/PBPP. It can be seen that the PER particles were not compatible with PP, and these were white points precipitation, attributed to the four hydroxyl groups in its structure. PEPA was easily agglomerated in PP, and there were still some holes around the particles of PEPA, which we suggested is because there is only one hydroxyl group in the structure of PEPA. PBPP was well dispersed in PP, and there were no agglomeration, due to no hydroxyl group in PBPP. All of these suggest that PBPP has a good compatibility with PP.

3.4. Compatibility of IFR with PP. Figure 6 shows the SEM images of IFR-PP (PER), IFR-PP (PEPA), and IFR-PP (PBPP). It can be seen that IFR containing PBPP had better compatibility than IFR containing PER and IFR containing PEPA. The interface between IFR (PBPP) and PP was

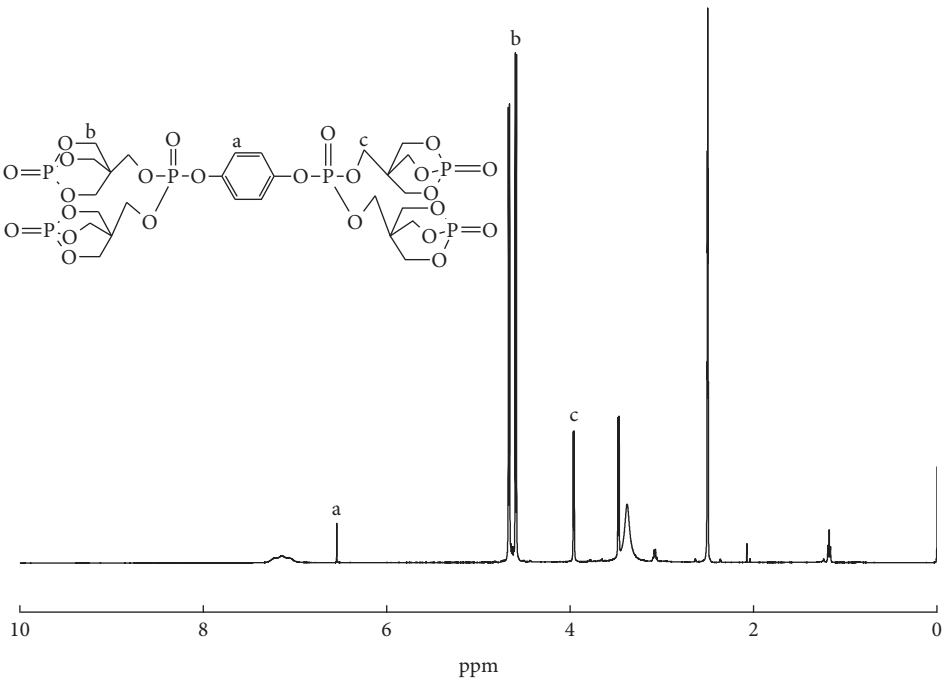

Figure 2: The ^{1}H NMR spectra of PBPP.

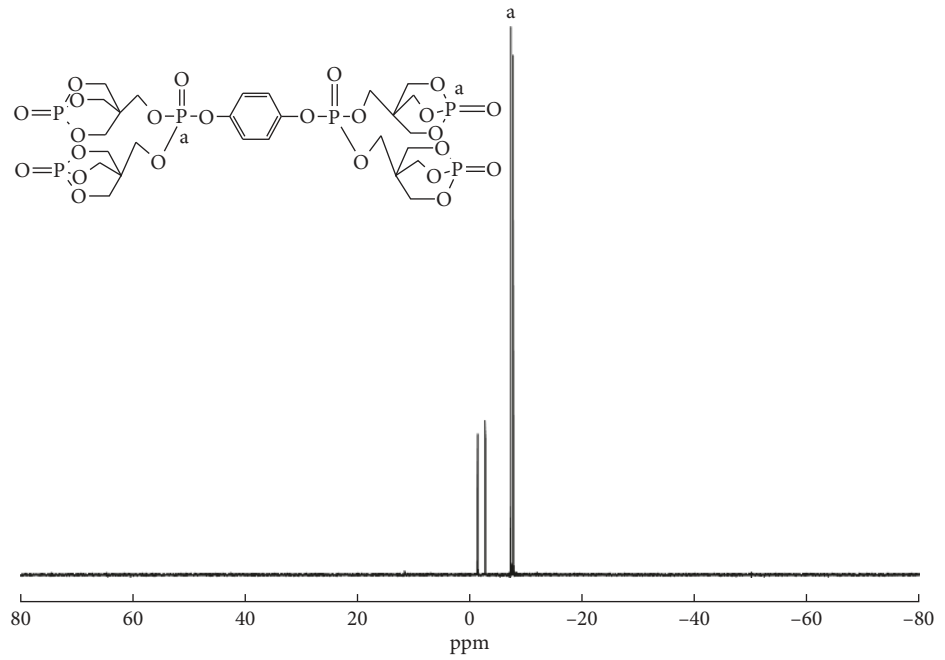

Figure 3: The ^{31}P NMR spectra of PBPP.

indistinct, and its surface was smooth and without any small holes. All of these suggest that IFR containing PBPP had better compatibility with PP.

3.5. Thermal Stability of PBPP, PEPA, and PER. Figure 7 shows TGA and DTG curves of PER, PEPA, and PBPP in air. The degradation processes of PBPP, PEPA, and PER each consisted of two steps. The first step of the degradation process of PBPP occurred between 350 and 370°C, with about 20% loss. The first step of the degradation of PEPA happened between 310 and 350°C down to 70% while that of PER occurred between 250 and 350°C with 84% or 95% loss, both of which started at lower temperature and had higher loss than PBPP. The temperatures of PBPP, PEPA, and PER for the second step of degradation were above 610°C, 530°C, and 360°C, respectively. It can be seen that PBPP had the highest temperature for the second step of the degradation

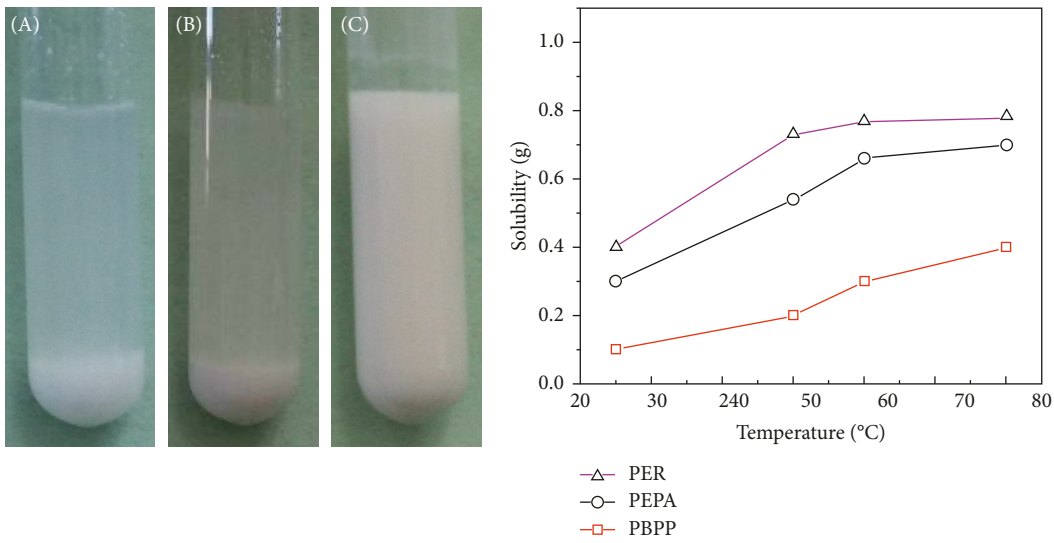

Figure 4: Digital photos and graphs of PER (A), PEPA (B), and PBPP (C) (1 g) dispersed in H_2O (5 ml) after standing for 2 h.

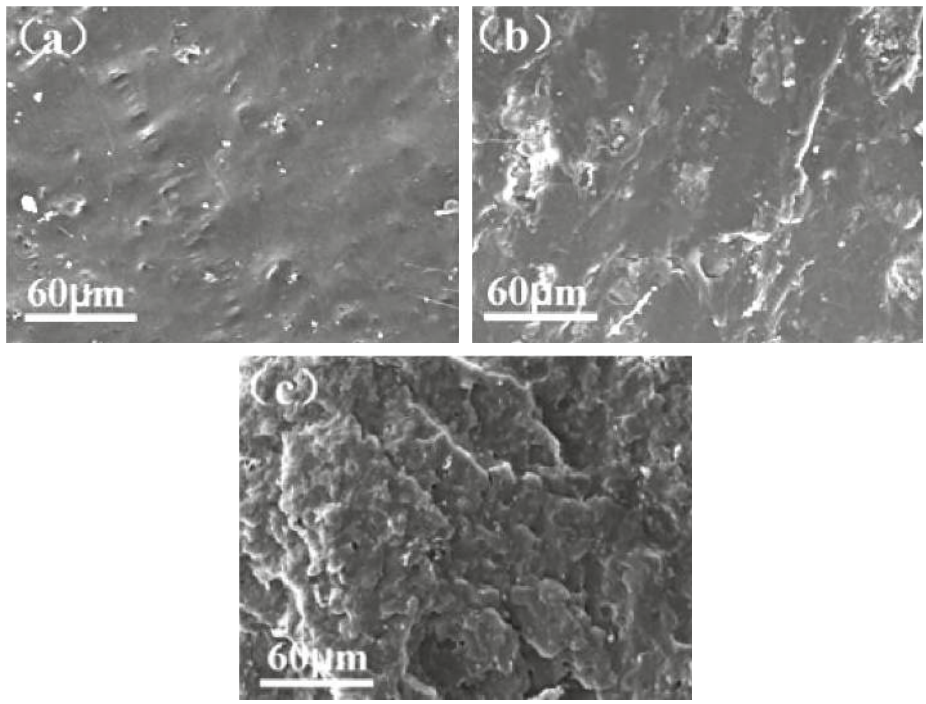

Figure 5: SEM (×500) of (a) PP/PER, (b) PP/PEPA, and (c) PP/PBPP.

process. Moreover, the char residue of PBPP was as high as 27% at 700°C, which was higher than the 15% of PEPA and 0.1% of PER. All of these show that the thermal stability of PBPP was higher than PEPA and PER. It is attributed to its symmetrical structure, stereohindrance effects, and the high carbon content of PBPP.

As can be seen in Figure 7(b), the thermal degradation processes of PER, PEPA, and PBPP had two steps based on the DTG profile. The degradation step of PBPP at 350°C can be assigned to the evolution of phosphoric acid. Moreover, PEPA showed a small peak in the range of 300–320°C, and PER showed a wide peak in the range of 250–350°C. All of these results have to be the same as the TGA ones and indicate that PBPP has good thermal stability.

3.6. Thermal Stability of IFR-PP Systems. Figure 8(a) shows the TG curves of the IFR-PP (PER), IFR-PP (PEPA), and IFR-PP (PBPP). The onset degradation temperature (T_{onset}) is defined as the temperature at which the weight loss is 5%. Comparing with the TGA results of the samples, T_{onset} of IFR-PP (PBPP) was 20°C higher than IFR-PP (PEPA) and 50°C

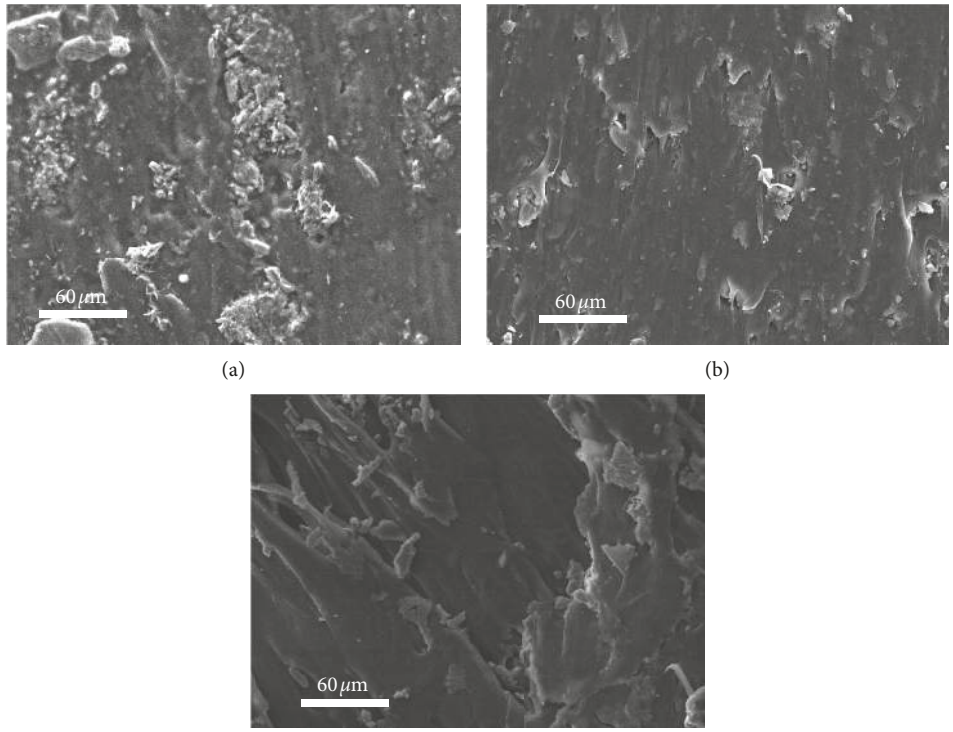

Figure 6: SEM (×500) of (a) IFR-PP (PER), (b) IFR-PP (PEPA), and (c) IFR-PP (PBPP).

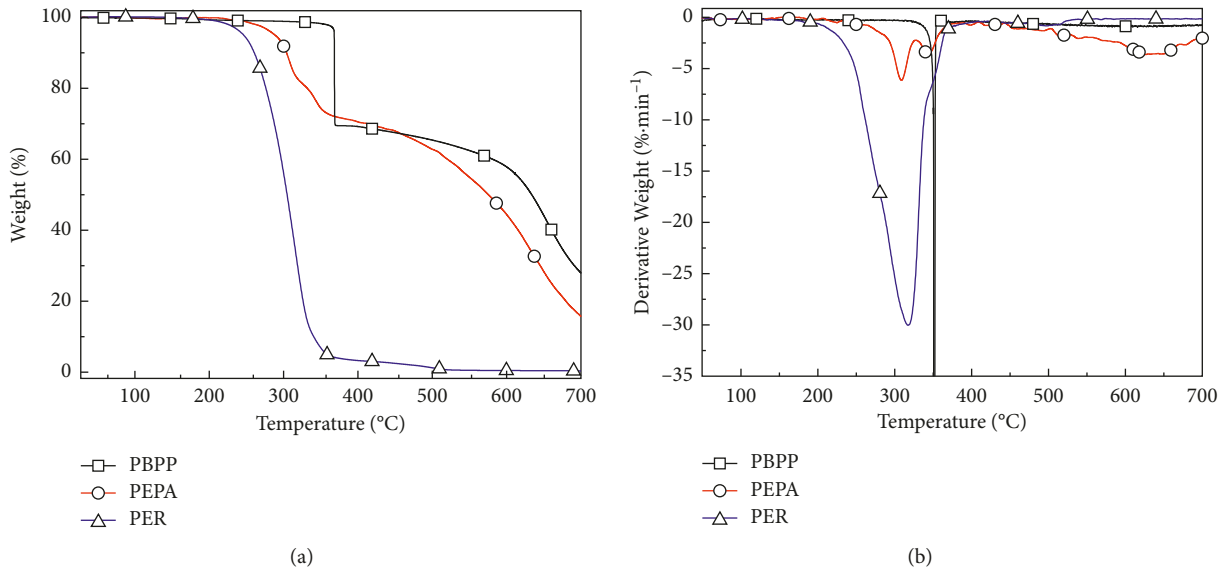

Figure 7: TG (a) and DTG (b) curves of PER, PEPA, and PBPP in air.

higher than IFR-PP (PER). The char residue of IFR-PP (PBPP) was 11% at 700°C which was 0.4% higher than IFR-PP (PEPA) and 4.4% higher than IFR-PP (PER). These experimental results further demonstrate that the IFR-PP system with PBPP has better thermal stability than that of PEPA or PER.

Figure 8(b) shows the DTG curves of the IFR-PP (PER), IFR-PP (PEPA), and IFR-PP (PBPP). It can be seen that the peak height of IFR-PP (PBPP) was 15% min^{-1}, which was similar to IFR-PP (PEPA), but 3% min^{-1} lower than IFR-PP (PER). By comparing the temperature of the peaks, it can be found that the maximum decomposed temperature of IFR-PP (PBPP) was higher than those of IFR-PP (PEPA) and IFR-PP (PER). The decomposed peak of IFR-PP (PBPP) was at 446°C, while that of IFR-PP (PEPA) was at 424°C and IFR-PP (PER) was at 434°C. The results further show IFR-PP (PBPP) had good thermal stability.

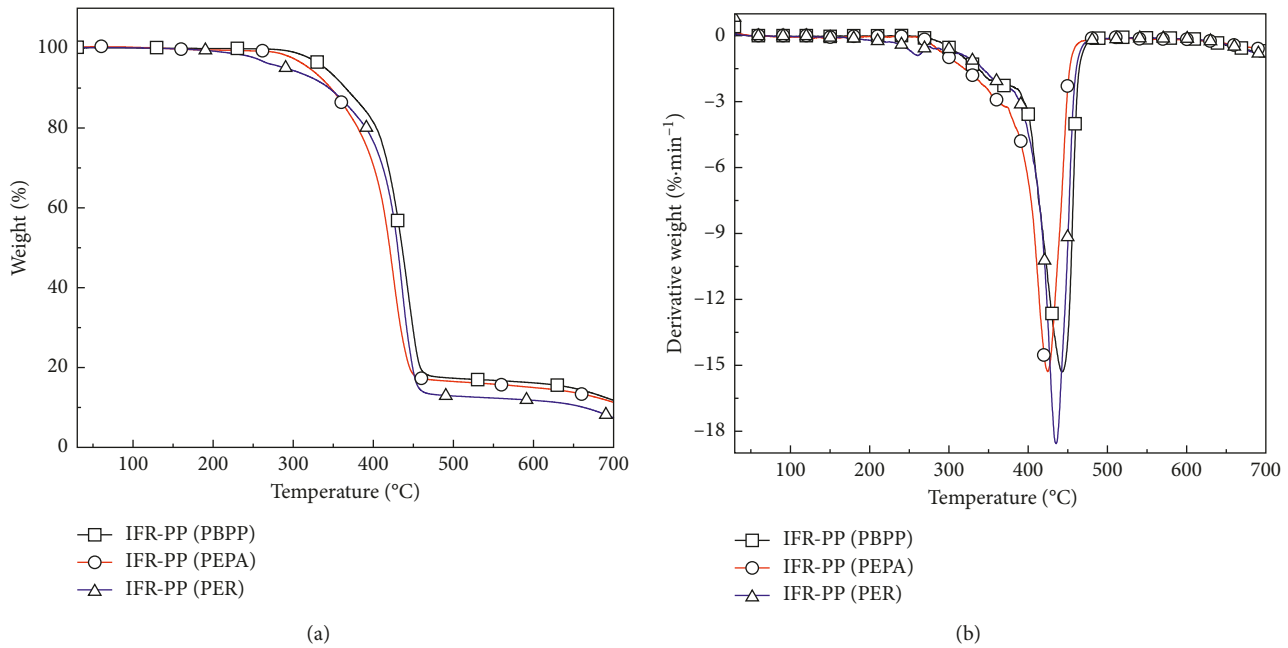

Figure 8: TG (a) and DTG (b) curves of IFR-PP with different charring agents in air.

Table 1: Effect of different ratios of APP to PBPP on flame retardancy of PP.

PP (g)	APP (g)	PBPP (g)	UL-94
100	0	0	V-2
75	25	0	V-2
75	20	5	V-1
75	15	10	V-0
75	10	15	V-0
75	5	20	V-2
75	0	25	V-2

Table 2: Effect of IFR addition on flame retardancy of PP.

Sample	PP (%)	IFR (%)	UL-94
IFR-PP (PER)	72	28	V-0
IFR-PP (PEPA)	72	28	V-0
IFR-PP (PBPP)	72	28	V-0
IFR-PP (PER)	75	25	V-2
IFR-PP (PEPA)	75	25	V-0
IFR-PP (PBPP)	75	25	V-0
IFR-PP (PER)	77	23	V-2
IFR-PP (PEPA)	77	23	V-0
IFR-PP (PBPP)	77	23	V-2

3.7. Flame Retardancy. Table 1 shows the vertical burning rates of the IFR-PP systems in which the addition of APP and PBPP totally accounted for 25% of the weight. Single additions of APP or PBPP showed little effect on the flame retardancy of PP. When PBPP was mixed with APP, the vertical burning rates of PP composites were better. When the weight ratio of APP to PBPP was 3 : 2 or 2 : 3, the vertical burning rates reached UL-94 V-0. However, for APP 25 or APP 20 and PBPP 5 (lack of the charring agent), APP 5 and PBPP 20 or PBPP 25(lack of the acid source) do not work mainly because the crosslinking between them is so weak that stable char layers cannot be formed for protecting inner PP during burning, and their vertical burning rates were V-2. The results of the vertical burning experiment showed that the optimal weight ratio of APP to PBPP was 3 : 2 or 2 : 3.

The UL-94 vertical burning tests are widely used to evaluate the flame retardant properties of materials. Table 2 lists the vertical burning rates for the IFR-PP (PBPP), IFR-PP (PEPA), and IFR-PP (PER). The experimental results showed that the flame retardant property of IFR-PP systems could reach V-0 when the minimal addition of IFR with PBPP, PEPA, or PER was 25%, 23%, and 28%, respectively. From the above results, it can be concluded that IFR-PP (PBPP) and IFR-PP (PEPA) can make a good performance in flame retardant PP. However, the addition of IFR-PP (PBPP) is 2% more than IFR-PP (PEPA), and it will not limit the application of IFR-PP (PBPP). The water resistance, compatibility, and thermal stability of IFR-PP (PBPP) are better than IFR-PP (PEPA), but its complexity of synthesis process limits its application in PP, and so, PEPA is more suitable for use in PP.

3.8. Cone Calorimeter Test. The combustion performance of the flame retardant materials has been evaluated by the cone calorimeter. The curves of the heat release rate (HRR), residual mass (mass), smoke production rate (SPR), and total smoke release (TSR) of the combustion behavior for IFR-PP (PER), IFR-PP (PEPA), and IFR-PP (PBPP) are shown in Figures 9 and 10.

It can be found from Figure 9(a) that there are two peaks that appeared in the HRR curves of IFR-PP (PER), IFR-PP (PEPA), and IFR-PP (PBPP). The width of the peak represents the burning time of all samples from the starting ignited time to the extinguishing time, and the IFR-PP(PER)

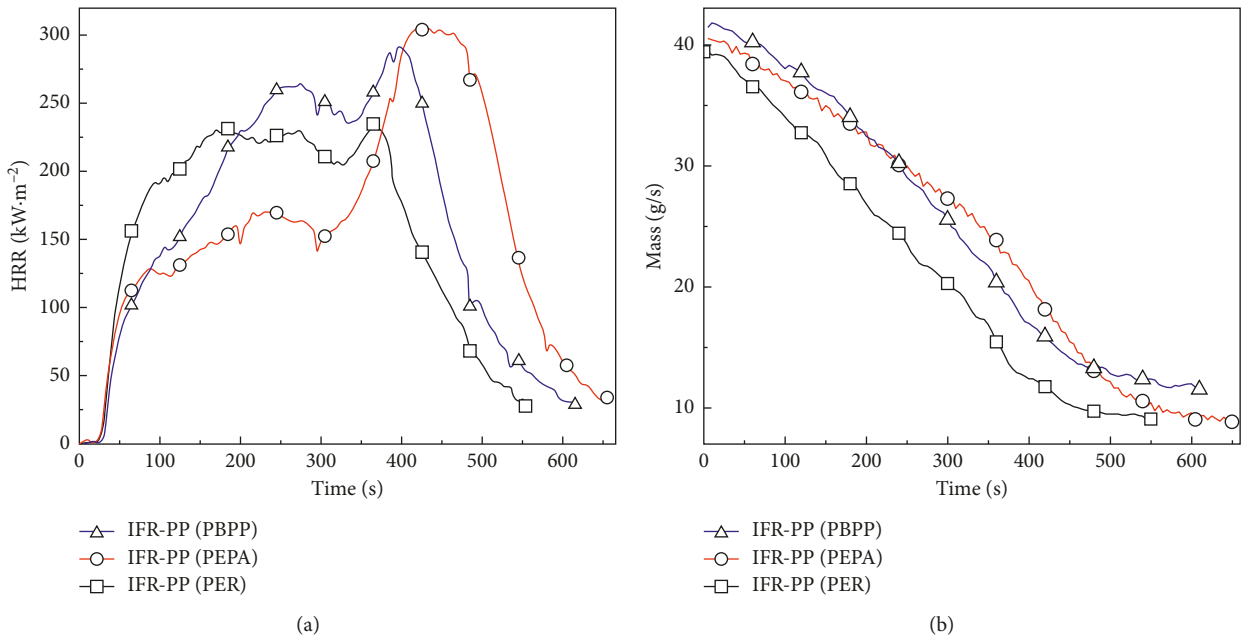

Figure 9: The HRR (a) and mass (b) curves of IFR-PP (PER), IFR-PP (PEPA), and IFR-PP (PBPP).

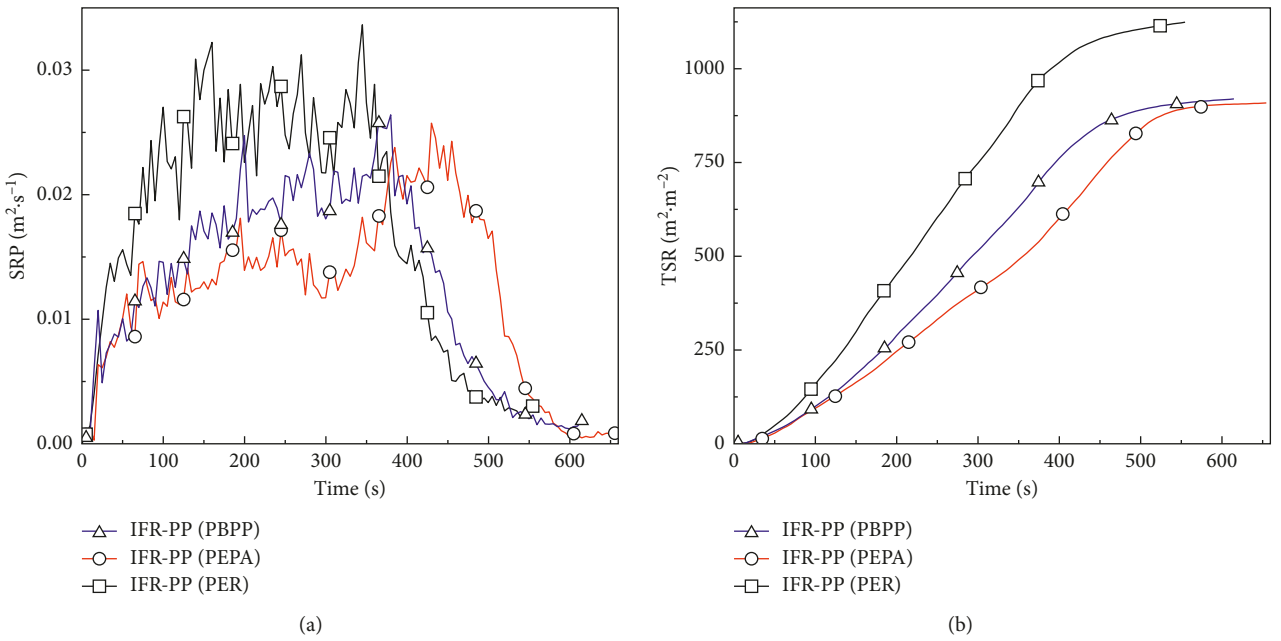

Figure 10: The SPR (a) and TSR (b) curves of IFR-PP (PER), IFR-PP (PEPA), and IFR-PP (PBPP).

combustion is prolonged to 550 s from 30 s, which lasts for 520 s; however, the IFR-PP(PEPA) and the IFR-PP(PBPP) are 620 s and 600 s separately, and the sequence of the burning time of the samples was IFR-PP (PEPA) > IFR-PP (PBPP) > IFR-PP (PER).

Figure 9(b) shows the residual mass (mass) curves of IFR-PP (PER), IFR-PP (PEPA), and IFR-PP (PBPP). Mass is a representative of the char residues of the material after burning. The char residue of IFR-PP (PBPP) was 12% at 555 s, which was higher than the char residues of IFR-PP (PEPA) and IFR-PP (PER), 9% and 8% at 555 s, respectively. This indicates that the residual mass of IFR-PP (PEPA) and IFR-PP (PER) is less than that of IFR-PP (PBPP) because the carbon content of PEPA and PER is less than that of PBPP.

The SPR and TSR curves are showed in Figures 10(a) and 10(b), respectively. It can be seen from Figure 10(a) that IFR-PP (PER) released more smoke and more quickly than IFR-PP (PBPP) and IFR-PP (PEPA). The peak of SPR for IFR-PP (PBPP) was the lowest among the three materials. Figure 10(b) showed the total smoke release of three different materials

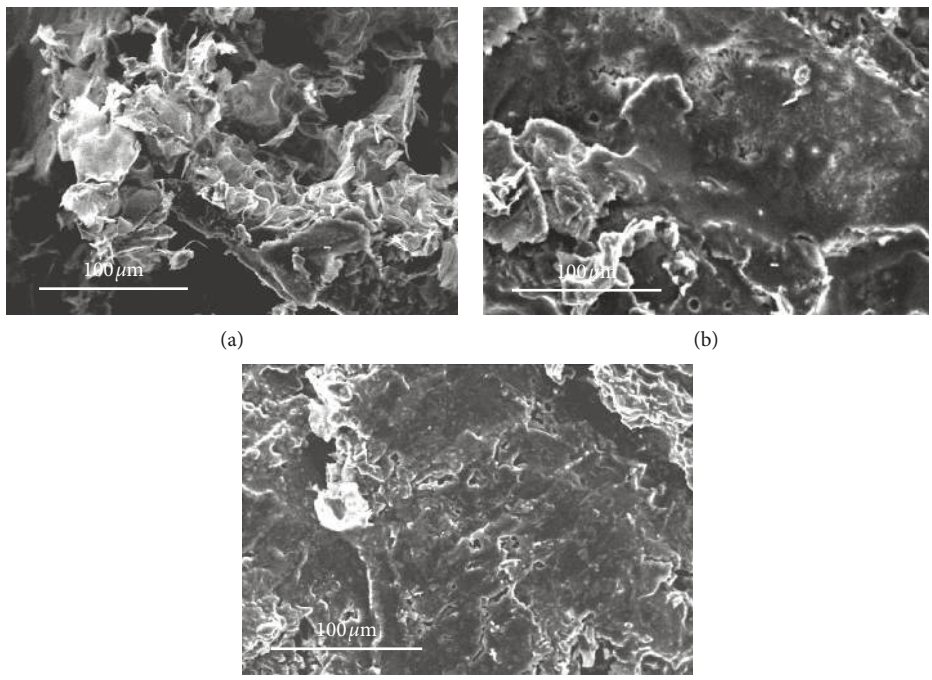

(a) (b)

(c)

Figure 11: SEM of the char layer (×250): (a) IFR-PP (PER); (b) IFR-PP (PEPA); and (c) IFR-PP (PBPP).

during burning, and the slope of IFR-PP (PBPP) was the lowest of the three materials. The results of SPR and TSR were related to the quality of the char layer of the three materials formed during burning.

3.9. Morphology of the Char Layer. The quality of the char layer is connected with its carbon content and compactness, and the compactness of the char layer is connected with the trend of forming a crosslinked char [28]. Figure 11 shows the SEM images of the residue char of IFR-PP (PER), IFR-PP (PEPA), and IFR-PP (PBPP) after the cone calorimeter tests. The surface of the char layer from IFR-PP (PEPA) was smoother and compacter than IFR-PP (PBPP) and IFR-PP (PER), which helps to prevent the transfer of heat and flammable volatiles and prevent the melted PP from dripping during combustion; however, there were many holes on the surface of the char layer of IFR-PP (PER), and this poor char layer could not prevent the degradation of the underlying PP and weakened the flame retardant effectiveness of IFR-PP (PER) in PP.

3.10. Flame Retardation Mechanism. In order to better understand the mechanism of intumescent flame retardant, Figure 12 shows the FT-IR spectra of the residual char of IFR-PP (PER), IFR-PP (PEPA), and IFR-PP (PBPP) heated at 300°C, 500°C, and after the cone calorimeter tests. Figure 13 is the proposed degradation mechanisms of IFR-PP (PER), IFR-PP (PEPA), and IFR-PP (PBPP). As can be seen in FT-IR at 300°C, there are peaks at 2938 cm^{-1} which are associated with -CH_2-. When the temperature increases to 500°C, the peaks at 2938 cm^{-1} disappeared in the FT-IR spectrum of the char of IFR-PP (PEPA) and IFR-PP (PER). This indicates that IFR-PP (PEPA) and IFR-PP (PER) were decomposed at 300°C but IFR-PP (PBPP) was still stable at 300°C.

At 500°C, the broad brands at 3444 cm^{-1} and 3143 cm^{-1} of IFR-PP (PBPP) (c) correspond to the stretching mode of -OH and the vibration of benzene rings, respectively, which are identical to the formulas of the degradation mechanism of IFR-PP (PBPP). The peaks at 1458 cm^{-1} of Figure 12(a) are attributed to the stretching mode of N-H in NH_4^+. Moreover, the absorption bands at 1400 cm^{-1} are assigned to P=O groups, and the peaks at 981 cm^{-1} are attributed to P-O in P-O-P groups in all three samples. Therefore, the FT-IR spectra of the residual char after the cone calorimeter tests confirm the existence of P-OH, P-O-P, P=O, and NH_4^+ groups in the char layers, which are identical to the degradation mechanism of IFR-PP (PBPP), IFR-PP (PEPA), and IFR-PP (PER). For the IFR-PP (PBPP), PBPP decomposes to benzoquinone and double-caged phosphate firstly, and then the double-caged phosphate reacts with ammonium polyphosphate to produce water and NH_3 secondly. With the temperature increasing, the charring agent finally forms the crosslinked char with the catalysis of phosphoric acid. Moreover, in the system of IFR-PP (PEPA), PEPA reacts with APP to form the crosslinked char directly which is similar to PER.

IFR-PP (PEPA) has the best performance in the flame retardant property, due to the hydroxy groups in the structure of PEPA, which can make the PEPA react with APP directly and form the crosslinked char. PBPP has a good performance as a flame retardant. Although there are not any hydroxy

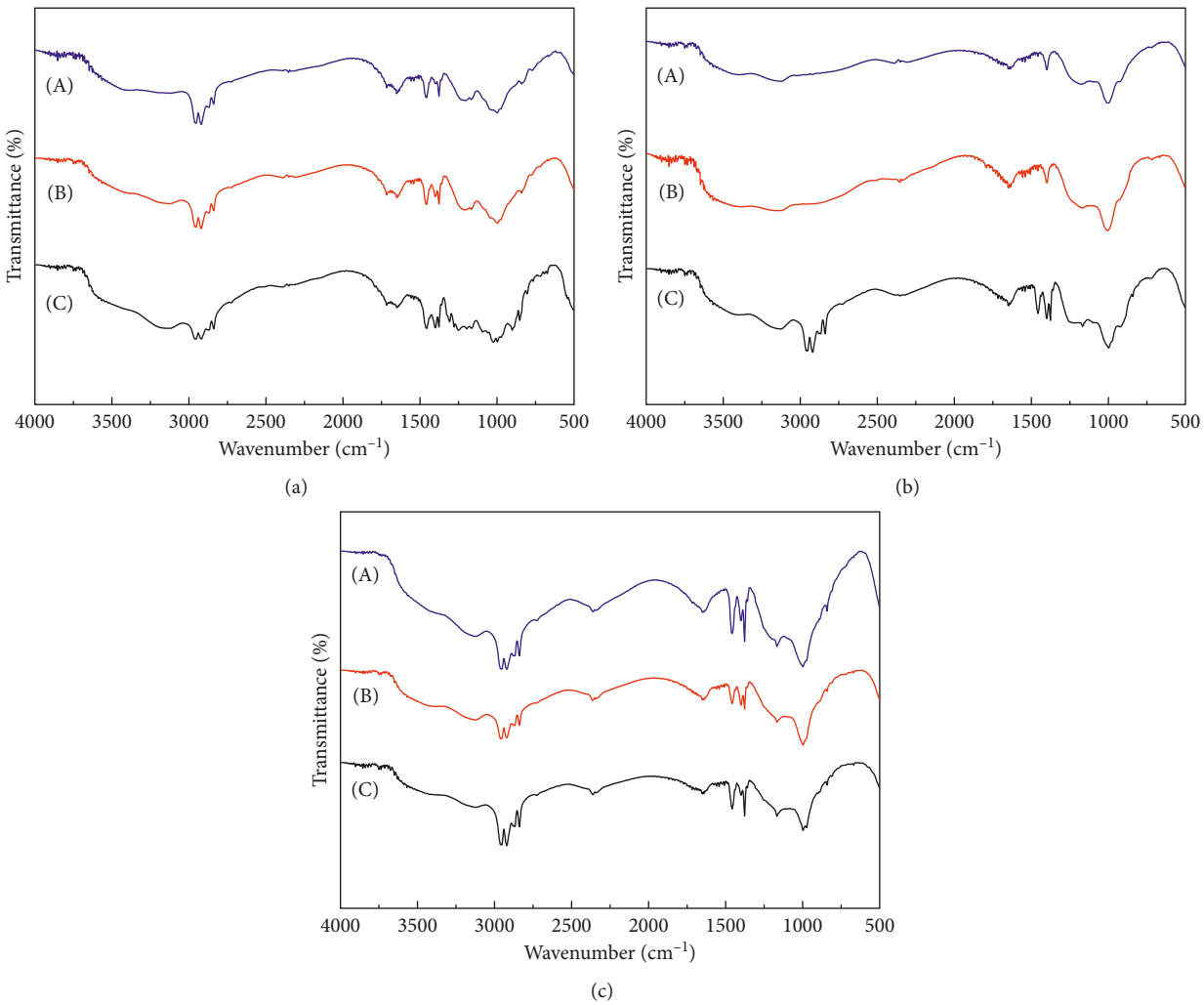

Figure 12: FT-IR spectra of char of IFR-PP (PER) (A), IFR-PP (PEPA) (B), and IFR-PP (PBPP) (C) in (a) 300°C, (b) 500°C, and (c) after cone calorimeter tests.

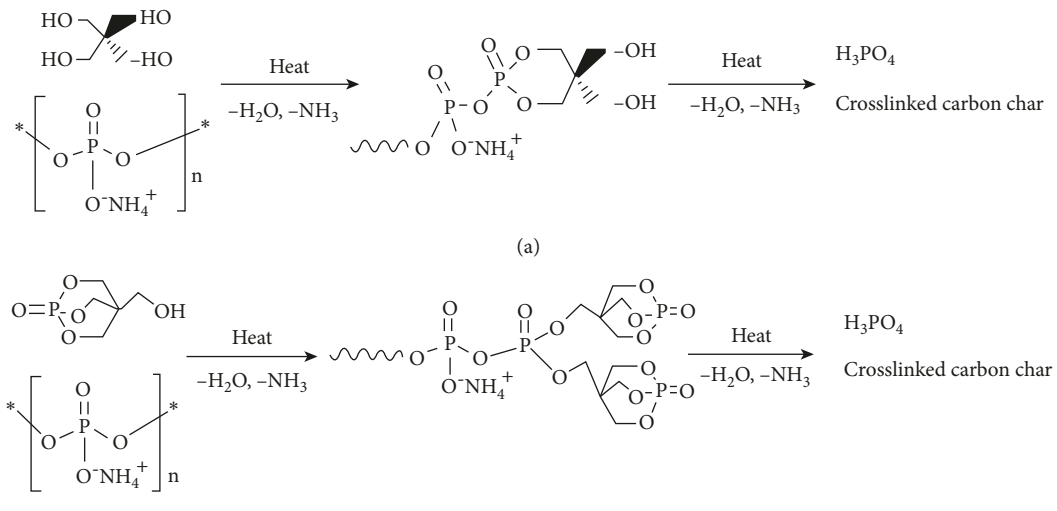

Figure 13: Continued.

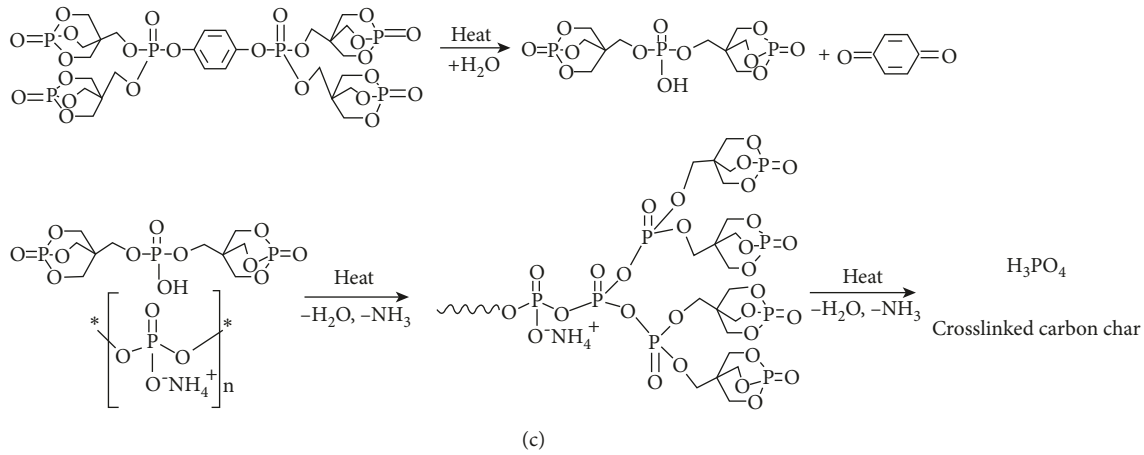

Figure 13: Formulas of the degradation mechanism of (a) IFR-PP (PER), (b) IFR-PP (PEPA), and (c) IFR-PP (PBPP).

groups in the structure of PBPP, however, it can decompose into a compound that contain two PEPA structures and a hydroxy group (Figure 13; formula (c)) and reacts with APP to form a crosslinked char, and at the same time, the high carbon content of PBPP can also help IFR-PP (PBPP) to form a char layer. IFR-PP (PER) can form a good crosslinked char by its four hydroxy groups, but its four hydroxyl groups also lead to poor compatibility with the PP matrix, and so, the quality of the char layer of IFR-PP (PER) formed during burning was poor. In a word, the flame retardant property of IFR on PP is IFR (PEPA) > IFR (PBPP) > IFR (PER).

4. Conclusions

(1) A charring agent (PBPP) containing two caged phosphates and benzene group was synthesized using PEPA, phosphorus oxychloride, and hydroquinone, and the structure of PBPP was characterized by FT-IR, ^{1}H NMR, and ^{31}P NMR.

(2) The effects of PBPP on water resistance, compatibility with PP, thermal stability, and flame retardant property for PP were compared to those of PEPA and PER. The experimental results showed that PBPP had a better performance in water resistance, compatibility with PP, thermal stability, and flame retardancy than PEPA and PER, attributed to its symmetrical structure and the stereohindrance effects of PBPP.

(3) Comparing the flame retardancy of IFR-PP (PBPP), IFR-PP (PEPA), and IFR-PP (PER) systems, the results show that the minimum additions of IFR-PP (PBPP), IFR-PP (PEPA), and IFR-PP (PER) needed for 25%, 23%, and 28%, respectively. Although the minimum needed addition of IFR-PP (PBPP) was slightly more than IFR-PP (PEPA), its comprehensive performance are better among the three charring agents.

(4) According to the SEM images of the residual char, the quality of the char layer of IFR-PP (PBPP) was good compared with IFR-PP (PEPA) and IFR-PP (PER) because IFR-PP (PBPP) can form an effective crosslinked char, and at the same time, the high carbon content of PBPP can also help IFR-PP (PBPP) to form a char layer.

Data Availability

The data used to support the findings of this study are available from the corresponding author upon request.

Conflicts of Interest

The authors declare that they have no conflicts of interest.

Acknowledgments

The authors wish to thank the financial supports from Guangdong Winner High-Tech & Industry Co. Ltd. and Science and Technology Department of Fushan City of Guangdong Province, China (no. 2016AG101374).

References

[1] H. Q. Peng, Q. Zhou, D. Y. Wang, L. Chen, and Y. Z. Wang, "A novel charring agent containing caged bicyclic phosphate and its application in intumescent flame retardant polypropylene systems," *Journal of Industrial and Engineering Chemistry*, vol. 14, no. 5, pp. 589–595, 2008.

[2] C. M. Feng, Y. Zhang, S. W. Liu, Z. G. Chi, and J. R. Xu, "Synthesis of novel triazine charring agent and its effect in intumescent flame-retardant polypropylene," *Journal of Applied Polymer Science*, vol. 123, no. 6, pp. 3208–3216, 2012.

[3] F. Zhang, P. F. Chen, and Y. Wang, "Smoke suppression and synergistic flame retardancy properties of zinc borate and diantimony trioxide in epoxy-based intumescent fire-retardant coating," *Journal of Thermal Analysis and Calorimetry*, vol. 123, no. 2, pp. 1319–1327, 2016.

[4] M. Q. Tang, F. Qi, and X. L. Chen, "Synergistic effects of ammonium polyphosphate and red phosphorus with expandable graphite on flammability and thermal properties of

HDPE/EVA blends," *Polymers for Advanced Technologies*, vol. 27, no. 1, pp. 52–60, 2016.

[5] J. Y. Xu, J. Liu, K. D. Li, L. Miao, and S. Tanemura, "Novel PEPA-functionalized graphene oxide for fire safety enhancement of polypropylene," *Science and Technology of Advanced Materials*, vol. 16, no. 2, pp. 1–11, 2015.

[6] L. Chen and Y. Z. Wang, "A review on flame retardant technology in China. Part I: development of flame retardants," *Polymers for Advanced Technologies*, vol. 21, pp. 1–26, 2010.

[7] S. Y. Liang, N. N. Matthias, and S. Gaan, "Recent developments in flame retardant polymeric coatings," *Progress in Organic Coatings*, vol. 76, no. 11, pp. 1642–1665, 2013.

[8] A. Dasari, Z. Z. Yu, G. P. Cai, and Y. W. Mai, "Recent developments in the fire retardancy of polymeric materials," *Progress in Polymer Science*, vol. 38, no. 9, pp. 1357–1387, 2013.

[9] S. Chiu and W. K. Wang, "Dynamic flame retardancy of polypropylene filled with ammonium polyphosphate, pentaerythritol and melamine additives," *Polymer*, vol. 39, no. 10, pp. 1951–1955, 1998.

[10] Q. Wu and B. J. Qu, "Synergistic effects of silicotungistic acid on intumescent flame-retardant polypropylene," *Polymer Degradation and Stability*, vol. 74, no. 2, pp. 255–261, 2001.

[11] Y. H. Chen, Y. Liu, Q. Wang, H. Yin, N. Aelmans, and R. Kierkels, "Performance of intumescent flame retardant master batch synthesized through twin-screw reactively extruding technology: effect of component ratio," *Polymer Degradation and Stability*, vol. 81, no. 2, pp. 215–224, 2003.

[12] P. Lv, Z. Z. Wang, L. Hu, and W. C. Fan, "Flammability and thermal degradation of flame retarded polypropylene composites containing melamine phosphate and pentaerythritol derivatives," *Polymer Degradation and Stability*, vol. 90, no. 3, pp. 523–534, 2005.

[13] X. C. Chen, Y. P. Ding, and T. Tang, "Synergistic effect of nickel formate on the thermal and flame-retardant properties of polypropylene," *Polymer International*, vol. 54, no. 6, pp. 904–908, 2005.

[14] Y. Tang, Y. Hu, S. F. Wang, Z. Gui, Z. Y. Chen, and W. C. Fan, "Intumescent flame retardant-montmorillonite synergism in polypropylene-layered silicate nanocomposites," *Polymer International*, vol. 52, no. 8, pp. 1396–1400, 2003.

[15] M. Bras, M. Bugajny, J. Lefebvre, and S. Bourbigot, "Use of polyurethanes as char-forming agents in polypropylene intumescent formulations," *Polymer International*, vol. 49, no. 10, pp. 1115–1124, 2000.

[16] Q. Li, H. F. Zhong, P. Wei, and P. K. Jiang, "Thermal degradation behaviors of polypropylene with novel silicon-containing intumescent flame retardant," *Journal of Applied Polymer Science*, vol. 98, no. 6, pp. 2487–2492, 2005.

[17] X. P. Hu, Y. L. Li, and Y. Z. Wang, "Synergistic effect of the charring agent on the thermal and flame retardant properties of polyethylene," *Macromolecular Materials and Engineering*, vol. 289, no. 2, pp. 208–212, 2004.

[18] F. Xie, Y. Z. Wang, B. Yang, and Y. Liu, "A novel intumescent flame-retardant polyethylene system," *Macromolecular Materials and Engineering*, vol. 291, no. 3, pp. 247–253, 2006.

[19] Z. L. Ma, M. Zhao, H. F. Hu, H. T. Ding, and J. Zhang, "Compatibilization of intumescent flame retardant/polypropylene composites based on α-methacrylic acid grafted polypropylene," *Journal of Applied Polymer Science*, vol. 83, no. 14, pp. 3128–3132, 2002.

[20] W. M. Zhu, E. D. Weil, and S. Mukhopadhyay, "Intumescent flame-retardant system of phosphates and 5,5,5′,5′,5″,5″-hexamethyltris(1,3,2-dioxaphosphorinanemethan)amine 2,2′,2″-trioxide for polyolefins," *Journal of Applied Polymer Science*, vol. 62, no. 13, pp. 2267–2280, 1996.

[21] G. Camino, L. Costa, and L. Trossarelli, "Study of the mechanism of intumescence in fire retardant polymers: part I-thermal degradation of ammonium polyphosphate-pentaerythritol mixtures," *Polymer Degradation and Stability*, vol. 6, no. 4, pp. 243–252, 1984.

[22] G. Camino, L. Costa, and L. Trossarelli, "Study of the mechanism of intumescence in fire retardant polymers: part II-mechanism of action in polypropylene ammonium polyphosphate pentaerythritol mixtures," *Polymer Degradation and Stability*, vol. 7, no. 1, pp. 25–31, 1984.

[23] G. Camino, L. Costa, and L. Trossarelli, "Study of the mechanism of intumescence in fire retardant polymers: part V-mechanism of formation of gaseous products in the thermal degradation of ammonium polyphosphate," *Polymer Degradation and Stability*, vol. 12, no. 3, pp. 203–211, 1985.

[24] N. Wang, G. Xu, Y. H. Wu et al., "The influence of expandable graphite on double-layered microcapsules in intumescent flame-retardant natural rubber composites," *Journal of Thermal Analysis and Calorimetry*, vol. 123, no. 2, pp. 1239–1251, 2016.

[25] G. Camino, N. Grassie, and I. C. McNeill, "Influence of the fire retardant, ammonium polyphosphate on the thermal degradation of poly(methyl methacrylate)," *Journal of Polymer Science: Polymer Chemistry Edition*, vol. 16, no. 1, pp. 95–106, 1978.

[26] W. Wang, Y. Peng, W. Zhang, and J. Li, "Effect of pentaerythritol on the properties of wood-flour/polypropylene/ammonium polyphosphate composite system," *BioResources*, vol. 10, no. 4, pp. 6917–6927, 2015.

[27] K. S. Lim, S. T. Bee, L. T. Sin et al., "A review of application of ammonium polyphosphate as intumescent flame retardant in thermoplastic composites," *Composites Part B: Engineering*, vol. 84, pp. 155–174, 2016.

[28] B. Li, C. Y. Sun, and X. C. Zhang, "An investigation of flammability of intumescent flame retardant polyethylene containing starch by using cone calorimeter," *Chemical Journal of Chinese Universities*, vol. 20, no. 1, pp. 146–149, 1999.

[29] G. J. Verkade, D. M. Nimrod, and R. D. Fitzwater, "The crystal structure of the bicyclic phosphate, 1-oxo-4-methyl-2,6,7-trioxa-1-phosphabicyclo[2.2.2] octane," *Journal of the American Chemical Society*, vol. 90, no. 11, pp. 2780–2784, 1968.

[30] Y. Halpern, D. M. Mott, and R. H. Niswander, "Fire retardancy of thermoplastic materials by intumescence," *Industrial & Engineering Chemistry Product Research and Development*, vol. 23, no. 2, pp. 233–238, 1984.

[31] Y. Z. Wang, B. Yi, B. Wu, B. Yang, and Y. Liu, "Thermal behaviors of flame-retardant polycarbonates containing diphenyl sulfone and poly(sulfonyl phenylene phosphonate)," *Journal of Applied Polymer Science*, vol. 89, no. 4, pp. 882–889, 2003.

[32] J. Chen, S. M. Liu, and J. Q. Zhao, "Synthesis, application and flame retardancy mechanism of a novel flame retardant containing silicon and caged bicyclic phosphate for polyamide-6," *Polymer Degradation and Stability*, vol. 96, no. 8, pp. 1508–1515, 2011.